JOURNAL OF GEOPHYSICAL RESEARCH, VOL. 94, NO. B1, PAGES 765–774, JANUARY 10, 1989

Source Type Plot for Inversion of the Moment Tensor

J. A. HUDSON

Department of Applied Mathematics and Theoretical Physics, Cambridge University, United Kingdom

R. G. PEARCE[1]

Section Applied Geophysics, Faculty of Mining and Petroleum Engineering, Delft University of Technology, The Netherlands

R. M. ROGERS[2]

Department of Geology, University of Wales, Cardiff, United Kingdom

Seismic signals provide information about the underlying moment tensor which, in turn, may be interpreted in terms of source mechanism. This paper is concerned with a two-dimensional graphical display of all possible relative sizes of the three principal moments; it provides a method of representing the probability density of these relative sizes deduced from a given set of data. Information provided by such a display, together with that relating to the orientation of the principal moments, provides as full a picture of the moment tensor as possible apart from an indication of its absolute magnitude. As with the compatibility plot, which was previously introduced to portray probability measures for different forms of P wave seismogram given a presumed source type, this "source type plot" for display of the principal moments is constructed to be "equal area" in the sense that the *a priori* probability density of the moment ratios is uniform over the whole plot. This *a priori* probability is based on the assumption that, with no information whatsoever concerning the source mechanism, each principal moment may independently take any value up to some arbitrary upper limit of magnitude, with equal likelihood. Although we have in mind the study of teleseismic relative amplitude data, the ideas can, in principle, be applied quite generally. The aim is to be able to display the degree of constraint imposed on the moment tensor by any set of observed data; estimates of the sizes of the principal moments together with their errors, when displayed on the source type plot, show directly the range of moment tensors compatible with the data.

1. INTRODUCTION

If we are to generalize the model of an earthquake source from the simple double couple mechanism, we must be quite clear what alternative assumption is to be made. Leaving aside the question of the time dependence of the source, it is customary to use a multipole expansion truncated after the first terms which do not violate conservation of linear and angular momentum [e.g., *Backus and Mulcahy*, 1976*a*, *b*]. These terms correspond to a linear combination of differently oriented source dipoles without moment, most easily represented by the moment tensor. This symmetric (3×3) tensor has six independent components providing six degrees of freedom. We take the view that it would be much more helpful to physical interpretation if six physically identifiable parameters were used rather than these six moment tensor components, and we endeavor to follow this approach.

In the end, the model should be capable of interpretation in terms of one or a combination of physical processes of failure resulting from an accumulated change in stress field. The processes may take any forms, e.g., shear or tensile fracture, explosion or implosion, each having an equivalent force system with its characteristic principal moments and each, in theory, distinguishable by its P and S radiation patterns. We therefore wish to ensure that the moment tensor is expressed in a way which separates as far as possible distinct types of physical mechanism. This means straightaway that the parameters describing the force system (which we refer to as the "source type") should be separated from those governing its orientation. The latter may be linked to the direction of the local stress field and of preexisting lines of weakness, but these are distinct from the question of the mechanism itself.

We achieve this separation of source type and orientation by diagonalizing the moment tensor; its three eigenvalues determine the mechanism, while the three angles defining the orientation of the principal axes complete the six parameters. In the case of a double couple fault rupture mechanism, the three angles chosen to represent the orientation of the source equate to the dip, strike, and slip angles [*Pearce*, 1977]. Although these angles cease to have the same physical meaning for other source types, they relate simply to the orientation in space of the moment eigenvectors and remain useful for comparing the orientation of alternative source types [*Pearce and Rogers*, this issue].

In choosing three physical parameters to define the source type, we first recognize that the principal moments

[1]Now at Department of Geology and Geophysics, University of Edinburgh, United Kingdom.

[2]Now at Ministry of Defence (Procurement Executive), Blacknest, Reading, United Kingdom.

Paper number 88JB03227.
0148–0227/89/88JB–3227$05.00

correspond only to the sizes of three orthogonal dipoles which constitute the source models, and these certainly do not relate to separate physical processes. Instead we choose two parameters T and k, which characterize the type of constant-volume (shear) component in the source, and the proportion of volume change component, respectively. The third parameter is then a scaling factor to fix the overall magnitude of the source; since we envisage the use of relative amplitude data, the absolute magnitude of the moments will be indeterminate, and this last parameter is discarded.

A source type can therefore be displayed on a two-dimensional diagram in terms of T and k. In order to show consistently the constraints imposed on the mechanism by any set of data (i.e., the restriction to a certain region of the T–k plane), we wish to construct a specific plot such that the *a priori* probability density for points on the display is uniform. In other words, if there is no prior knowledge of, or preference for, a specific source type, the probability of source types corresponding to a range of (T, k) points lying within a certain region of the plot is directly proportional to the area of that region alone. We describe this equal-area representation as the "source type plot."

For orientation, the choice of distribution corresponding to minimum *a priori* constraint is simple: with no prior information, every orientation is equally likely [see *Pearce*, 1979, 1980]. For source type, we specify that the values of the three principal moments are independent and uniformly distributed in $[-L, L]$, where L is an arbitrary upper limit. Since we are not concerned with absolute magnitudes, the actual value of L is irrelevant.

In this way the size of the region to which the values of T and k are constrained by the data gives a quantitative measure of the accuracy of the measurement of source type, unaffected by the particular choice of parameterization.

2. Parametric Representation of the Moment Tensor

The diagonalized moment tensor may in all cases be decomposed into an isotropic and a nonisotropic part. The isotropic part may be specified by a single scalar and corresponds to pure dilatation at the source, while the nonisotropic component requires two parameters to define its size and type, and corresponds to a mechanism without volume change. We choose the parameter k as a measure of the relative size of the dilatational component, the corresponding size of the constant-volume component being $(1-|k|)$. We then use T as a second parameter to define the form of the constant-volume component. The third parameter, if included, would define the absolute source size.

Previous authors have used the relative size of two orthogonal double couples, or the relative sizes of a double couple and a compensated linear vector dipole (CLVD) as a means of expressing the nature of the constant-volume component [e.g., *Knopoff and Randall*, 1970; *Fitch et al.*, 1980]. Although they may be mathematically convenient, there are any number of ways of achieving such decompositions, and they do not in general correspond to any physical components of the source.

The choice of k, the proportion of dilatational component, as an explicit parameter is a natural outcome of our decision to separate orientation from source type; only the constant-volume component of source type is affected by orientation. Moreover, explosive component is of specific interest; the dilatational model is the one normally used for an explosive source, which is one source type known to occur on its own, or which alternatively may accompany a (conceptually) separate constant-volume mechanism.

Although it is less clear what would represent the most physically justifiable choice of constant-volume parameter, the double couple is one constant-volume mechanism known to occur on its own, and we define our parameter T such that it passes through the double couple to include all other types of constant-volume component, with the same orientation of principal stress axes. The mechanisms most different from the double couple are the positive and negative CLVDs, which accordingly correspond to the numerically extreme values of T. Therefore although T in fact corresponds numerically to the relative sizes of a notional negative CLVD and a double couple similarly oriented, we shall consider the parameter as simply the characteristic of the single constant-volume component.

Some authors [e.g., *Dziewonski et al.*, 1981] express the six moment tensor components with respect to a vertical set of axes, a representation which is not explicit in either source type or orientation. The principal moments, which are also given, are only interpretable in terms of source type by examining the relationship between their numerical values. The percentage deviation from a double couple, or the best fit double couple, gives this one source type a special significance and does not provide an informative measure of the confidence in terms of either the source type itself or its orientation. The parametric representation which we develop here is, we believe, both economical and informative.

So that the orientation of the moment tensor shall be uniquely defined, we order the relative sizes of the three principal moments M_x, M_y, and M_z; that is, for any specified orientation the smallest, intermediate, and largest principal axes are in the same directions for all source types. This is important when considering the causative stress field, and is done without loss of generality. We begin therefore with the ordering

$$M_x \geq M_z \geq M_y \tag{1}$$

and define the isotropic part M, where

$$3M = M_x + M_y + M_z \tag{2}$$

and the deviatoric moments

$$M_x' = M_x - M \quad M_y' = M_y - M \quad M_z' = M_z - M \tag{3}$$

The dilatational component of the moment tensor is, of course, represented by M, while M_x', M_y', and M_z' determine the constant-volume component. We begin scaling by taking the ratio of each moment to one of their number. In order to avoid the danger of division by zero, we separate the possible cases into $M_z' > 0$, $M_z' = 0$, and $M_z' < 0$.

If $M'_z > 0$ it follows that $M'_y < 0$ (since $M'_x + M'_y + M'_z = 0$ and $M'_x \geq M'_z \geq M_y$). We now scale all moments by $(-2/M'_y)$:

$$\overline{M}_x = -2M_x/M'_y \quad \overline{M}'_x = -2M'_x/M'_y \ \ldots$$
$$\overline{M} = -2M/M'_y \tag{4}$$

where the overbar indicates the scaling. We see that

$$\overline{M}'_y = -2$$
$$0 < \overline{M}'_z = \frac{-2M'_z}{M'_y} = \frac{2M'_z}{M'_x + M'_z} \leq 1$$
$$\overline{M}'_x = \frac{-2M'_x}{M'_y} = 2 - M'_z \tag{5}$$

so the deviatoric part $\mathrm{diag}\{M'_x, M'_y, M'_z\}$ of the moment tensor may be separated into two parts:

$$\mathrm{diag}\{\overline{M}'_x, \overline{M}'_y, \overline{M}'_z\} = 2\,\mathrm{diag}\{1, -1, 0\} + \overline{M}'_z\,\mathrm{diag}\{-1, 0, 1\} \tag{6}$$

We define our first parameter T therefore by

$$T = \overline{M}'_z = -2(M'_z/M'_y) \quad 0 < T \leq 1 \tag{7}$$

so that

$$\overline{M}'_x = 2 - T \quad \overline{M}'_y = -2 \quad \overline{M}'_z = T \tag{8}$$

The second parameter k is chosen to measure the dilatational component. We put

$$\overline{M} = 2k/(1-|k|) \quad -1 < k < 1 \tag{9}$$

or $k = \overline{M}/(2+|\overline{M}|)$ and scale by the factor $2k/\overline{M}$ or, equivalently, by $(1-|k|)$, so that

$$\overline{\overline{M}}_x = 2k\,\overline{M}_x/\overline{M} = 2kM_x/M \ \ldots$$
$$\overline{\overline{M}} = 2k \tag{10}$$

where the double overbar indicates the new scaling.

If $\overline{M} = 0$, $k = 0$, and the factor $2k/\overline{M}$ reduces to unity (as $(1-|k|)$ obviously does) and the scaling is by unity. Finally, we have

$$\overline{\overline{M}}_x = 2k + (1-|k|)(2-T)$$
$$\overline{\overline{M}}_y = 2k - 2(1-|k|)$$
$$\overline{\overline{M}}_z = 2k + T(1-|k|) \tag{11}$$

In the case $M'_z < 0$, then $M'_x > 0$, and we begin by scaling by $(2/M'_x)$ (instead of $(-2/M'_y)$), so that

$$\overline{M}'_x = 2$$
$$\overline{M}'_z = 2M'_z/M'_x \quad -1 \leq \overline{M}'_z < 0$$
$$\overline{M}'_y = 2M'_y/M'_x = -2 - \overline{M}'_z \tag{12}$$

Again we define

$$T = \overline{M}'_z \quad -1 \leq T < 0 \tag{13}$$

and k as before, according to (9). Scaling once again by $2k/\overline{M}$ (or, equivalently, by $(1-|k|)$), or by unity if $\overline{M} = k = 0$, we have

$$\overline{\overline{M}} = 2k$$
$$\overline{\overline{M}}_x = 2k + 2(1-|k|)$$
$$\overline{\overline{M}}_y = 2k - (2+T)(1-|k|)$$
$$\overline{\overline{M}}_z = 2k + T(1-|k|) \tag{14}$$

Finally, if $M'_z = 0$, we have $M'_x = -M'_y$ and, assuming these two components are nonzero, we scale by $(2/M'_x) = (-2/M'_y)$ again, so that

$$\overline{M}'_x = -\overline{M}'_y = -2 \tag{15}$$

This time we put $T = 0$, since it corresponds to the limiting value of T as M'_y tends to zero from either above or below, and define k according to (9) again. Scaling by $(2k/\overline{M})$, or by unity if $\overline{M} = k = 0$, we have

$$\overline{\overline{M}} = 2k$$
$$\overline{\overline{M}}_x = 2k + 2(1-|k|) = -\overline{\overline{M}}_y$$
$$\overline{\overline{M}}_z = 2k \tag{16}$$

If, in addition to $M'_z = 0$, we have $M'_x = 0 = M'_y$, we define $k = M/|M|$ (as the unambiguous limiting value of k as M'_x and M'_y tend to zero) and scale by $2k/M$ (that is, $2/|M|$) again to get

$$\overline{\overline{M}}_x = \overline{\overline{M}}_y = \overline{\overline{M}}_z = 2k \tag{17}$$

In summary, we have defined two parameters in terms of the ordered principal moments M_x, M_z, and M_y:

$$\begin{aligned} k &= M/(|M| - M'_y) \quad M'_z \geq 0 \\ k &= M/(|M| + M'_x) \quad M'_z \leq 0 \end{aligned} \qquad -1 \leq k \leq 1 \tag{18}$$

and

$$\begin{aligned} T &= -2M'_z/M'_y \quad M'_z > 0 \quad 0 < T \leq 1 \\ T &= 0 \quad M'_z = 0 \\ T &= 2M'_z/M'_x \quad M'_z < 0 \quad -1 \leq T < 0 \end{aligned} \tag{19}$$

The combined scaling factor is, in every case,

$$\frac{2k}{M}=\frac{2}{|M|-M'_y} \quad M'_z \geq 0$$
$$\frac{2k}{M}=\frac{2}{|M|+M'_x} \quad M'_z \leq 0 \qquad (20)$$

and the scaled moments are

$$\overline{\overline{M}}_x = 2k+(2-T)(1-|k|) \quad T \geq 0$$
$$\overline{\overline{M}}_y = 2k-2(1-|k|)$$
$$\overline{\overline{M}}_x = 2k+2(1-|k|) \quad T \leq 0$$
$$\overline{\overline{M}}_y = 2k-(2+T)(1-|k|)$$
$$\overline{\overline{M}}_z = 2k+T(1-|k|)$$
$$\overline{\overline{M}} = (\overline{\overline{M}}_x+\overline{\overline{M}}_y+\overline{\overline{M}}_z)/3 = 2k \qquad (21)$$

where both T and k lie in the range [−1, 1]. Every moment tensor can be presented in this form with unique values of T and k, and it is used by *Pearce and Rogers* [this issue, equation (1)].

We see that the dilatational component is given by $\overline{M} = 2k$, varying from −2 to +2, and the nonisotropic constant-volume component is given by the deviatoric moments

$$\overline{\overline{M}}'_x = (1-|k|)(2-T) \quad T \geq 0$$
$$\overline{\overline{M}}'_y = (1-|k|)(-2)$$
$$\overline{\overline{M}}'_x = (1-|k|)(2) \quad T \leq 0$$
$$\overline{\overline{M}}'_y = (1-|k|)(-2-T)$$
$$\overline{\overline{M}}'_z = (1-|k|)(T) \quad -1 \leq T \leq 1 \qquad (22)$$

3. *A Priori* Probability Distribution for T and k

We base the *a priori* probability distribution of the principal moments on the assumption that, before any account is taken of possible source models, each principal value of the moment tensor can be considered as a random variable m, independent of the other two and having a probability density function $\phi(X)$ $(-\infty < X < \infty)$, the same for each principal moment. This assumption is, of course, not based on any observation but is designed as a basis with respect to which the observed probability density of source types can be measured.

Without loss of generality and following (1), we choose M_x as the principal moment with the highest value, so

$$\Pr\{M_x \in [X, X+dX]\}$$
$$= 3\Pr\{m \in [X, X+dX]\} \times (\Pr\{m \in [-\infty, X]\})^2$$
$$= 3\phi(X)\ \Phi^2(X)dX \qquad (23)$$

where $\Phi(X)$ is the cumulative probability function given by

$$\Phi(X) = \int_{-\infty}^{X} \phi(m)dm \qquad (24)$$

Thus the probability density for M_x is

$$\phi_x(X) = 3\phi(X)\ \Phi^2(X)$$

Similarly, since we choose M_y to be the moment with the lowest value,

$$\Pr\{M_y \in [X, X+dX]\}$$
$$= 3\phi(X)\ (1-\Phi(X))^2 dX = \phi_y(X)dX \qquad (25)$$

and

$$\Pr\{M_z \in [X, X+dX]\}$$
$$= 3\phi(X)\ \Phi(X)\ (1-\Phi(X))dX = \phi_z(X)dX \qquad (26)$$

We wish to find the combined probability distribution for T and k. Suppose, first of all, that $0 < k < 1$, $0 < T < 1$; then $M > 0$, $M'_z > 0$, and (equations (18) and (19))

$$k = \frac{M}{2M-M_y} \quad T = \frac{-2(M_z-M)}{M_y-M}$$

The scaled values of M_x, M_y, and M_z are given by (21). Replacing the scaling factor $(M/2k)$, we have

$$M_x = \frac{M}{2k}[2-T(1-k)]$$
$$M_y = \frac{M}{2k}[4k-2]$$
$$M_z = \frac{M}{2k}[2k+T(1-k)] \qquad (27)$$

We now define two new parameters μ and τ:

$$\mu = \frac{M}{2k} \quad \tau = T(1-|k|) \qquad (28)$$

so that

$$M_x = \mu(2-\tau) \quad M_y = 2\mu(2k-1) \quad M_z = \mu(2k+\tau) \qquad (29)$$

with $0 < \mu < \infty$, $0 < \tau < 1-k$, and $0 < k < 1$.

The substitution of τ for T makes each moment linear in τ and k for each different value of μ, and we look for a combined probability distribution for τ and k in the first instance. The combined probability distribution for M_x, M_y, and M_z taking values X, Y, and Z respectively, $(X \geq Z \geq Y)$ is

$$6\ \phi(X)\ \phi(Y)\ \phi(Z) \qquad (30)$$

where the factor 6 corresponds to the six ways of choosing the coordinate axes as the X, Y, and Z axes. It follows that the probability density function for τ, k, and μ is

$$6\,\phi(X)\,\phi(Y)\,\phi(Z)\left|\frac{\partial(X,Y,Z)}{\partial(\tau,k,\mu)}\right| \tag{31}$$

where $X=\mu(2-\tau)$, $Y=2\mu(2k-1)$, $Z=\mu(2k+\tau)$, and

$$\frac{\partial(X,Y,Z)}{\partial(\tau,k,\mu)}$$

is the Jacobian

$$\begin{vmatrix} \frac{\partial X}{\partial\tau} & \frac{\partial X}{\partial k} & \frac{\partial X}{\partial\mu} \\ \frac{\partial Y}{\partial\tau} & \frac{\partial Y}{\partial k} & \frac{\partial Y}{\partial\mu} \\ \frac{\partial Z}{\partial\tau} & \frac{\partial Z}{\partial k} & \frac{\partial Z}{\partial\mu} \end{vmatrix} = \begin{vmatrix} -\mu & 0 & 2-\tau \\ 0 & 4\mu & 4k-2 \\ \mu & 2\mu & 2k+\tau \end{vmatrix} = -12\mu^2 \tag{32}$$

The combined distribution of τ and k is therefore

$$\psi(\tau,k)=6\int_0^\infty \phi(X)\,\phi(Y)\,\phi(Z)\left|\frac{\partial(X,Y,Z)}{\partial(\tau,k,\mu)}\right|d\mu$$

$$=72\int_0^\infty \phi\{\mu(2-\tau)\}\,\phi\{2\mu(2k-1)\}\,\phi\{\mu(2k+\tau)\}\,\mu^2 d\mu \tag{33}$$

If $0<T<1$, and $-1<k<0$, then $M<0$ and $M_z'>0$. The same formulae hold as before but with

$$X=\mu(2+4k-\tau) \quad Y=-2\mu \quad Z=\mu(2k+\tau) \tag{34}$$

and

$$\frac{\partial(X,Y,Z)}{\partial(\tau,k,\mu)}=\begin{vmatrix} -\mu & 4\mu & 2+4k-\tau \\ 0 & 0 & -2 \\ \mu & 2\mu & 2k+\tau \end{vmatrix}=-12\mu^2$$

So

$$\psi(\tau,k)$$
$$=72\int_0^\infty \phi\{\mu(2+4k-\tau)\}\,\phi(-2\mu)\,\phi\{\mu(2k+\tau)\}\,\mu^2 d\mu$$
$$0<\tau<1+k \quad -1<k<0 \tag{35}$$

If, now, $-1<T<0$ and $0<k<1$, then $M>0$ and $M_z'<0$;

$$X=2\mu \quad Y=\mu(-2+4k-\tau) \quad Z=\mu(2k+\tau) \tag{36}$$

and

$$\frac{\partial(X,Y,Z)}{\partial(\tau,k,\mu)}=-12\mu^2$$

again. Hence

$$\psi(\tau,k)$$
$$=72\int_0^\infty \phi(2\mu)\,\phi\{\mu(-2+4k-\tau)\}\,\phi\{\mu(2k+\tau)\}\,\mu^2 d\mu$$
$$-(1-k)<\tau<0 \quad 0<k<1 \tag{37}$$

Finally, if both τ and k are negative, then so are M and M_z', and

$$X=\mu(4k+2) \quad Y=\mu(-2-\tau) \quad Z=\mu(2k+\tau)$$
$$\frac{\partial(X,Y,Z)}{\partial(\tau,k,\mu)}=-12\mu^2 \tag{38}$$

and so

$$\psi(\tau,k)$$
$$=72\int_0^\infty \phi\{\mu(4k+2)\}\,\phi\{\mu(-2-\tau)\}\,\phi\{\mu(2k+\tau)\}\,\mu^2 d\mu$$
$$-(1+k)<\tau<0 \quad -1<k<0 \tag{39}$$

Equations (33), (35), (37), and (39) give $\psi(\tau,k)$ for the whole range of relevant values of τ and k except for the endpoint values e.g., $k=-1, 0, 1$. These can be found as limiting values of the given expressions.

The corresponding distribution function $\Psi(T,k)$ for T and k can be found directly from $\psi(\tau,k)$ from the formula

$$\Psi(T,k)=\psi(\tau,k)\left|\frac{\partial(\tau,k)}{\partial(T,k)}\right|=\psi(\tau,k)\,(1-|k|) \tag{40}$$

We now propose our simple model for $\phi(X)$, the *a priori* probability distribution for each principal moment, and one expressing almost total lack of information. As proposed earlier, we assume ϕ to be constant between positive and negative limits $\pm L$ ($L>0$):

$$\phi(X)=\frac{L}{2} \quad |X|\le L$$
$$\phi(X)=0 \quad |X|>L \tag{41}$$

Since we scale the moments and pay no attention to absolute magnitude, the value of L is irrelevant to the distribution of T and k.

It follows, for instance, that the probability density function for the ordered moments M_x, M_z, and M_y are (equations (23), (25), and (26))

$$\phi_x(X)=\frac{3}{8L^3}(L+X)^2$$
$$\phi_y(X)=\frac{3}{8L^3}(L-X)^2 \qquad |X|\le L$$
$$\phi_z(X)=\frac{3}{8L^3}(L^2-X^2)$$

$$\phi_x(X)=\phi_y(X)=\phi_z(X)=0 \quad |X|>L \tag{42}$$

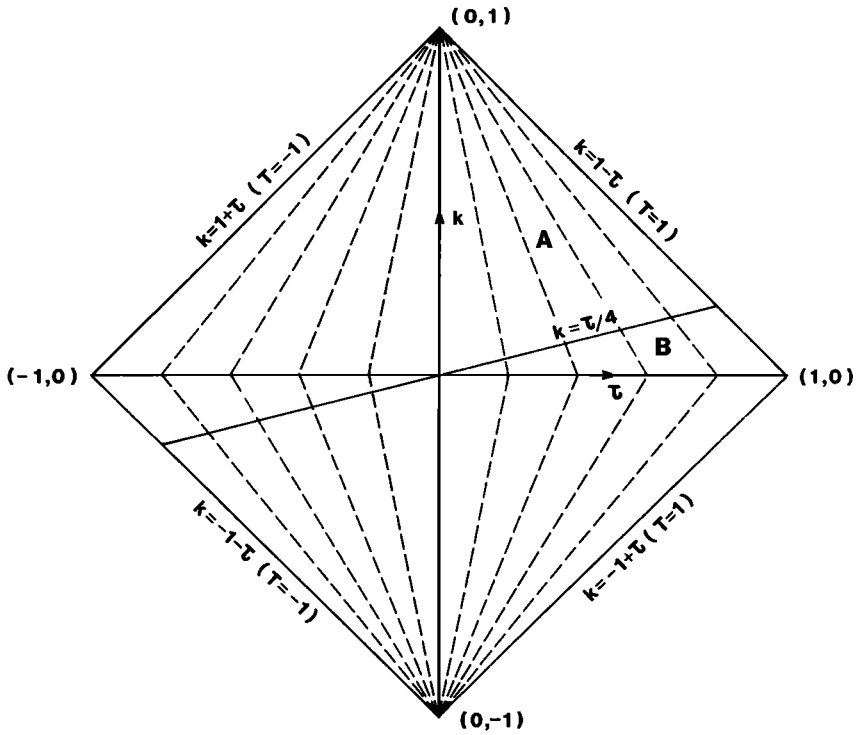

Fig. 1. Representation of source types using the parameters T and k plotted in the τ–k plane (see text). Lines of equal T are shown pecked; lines of equal k are horizontal and equally spaced.

The combined distribution of τ and k in the first quadrant ($0 < \tau < 1-k$, $0 < k < 1$) is (equation (33))

$$\psi(\tau, k) = \frac{9}{L^3}\int_0^{L/\xi} \mu^2 d\mu = \frac{3}{\xi^3} \tag{43}$$

where

$$\xi = \max\{2-\tau, 2-4k\}$$

That is,

$$\psi(\tau, k) = \frac{3}{(2-\tau)^3} \qquad \tau \le 4k$$
$$\psi(\tau, k) = \frac{3}{8(1-2k)^3} \qquad \tau \ge 4k \tag{44}$$

(see Figure 1).

Similarly, in the third quadrant ($-(1+k) < \tau < 0$, $-1 < k < 0$)

$$\psi(\tau, k) = \frac{9}{L^3}\int_0^{L/\eta} \mu^2 d\mu = \frac{3}{\eta^3} \tag{45}$$

(from (39)), where

$$\eta = \max\{2+\tau, 2+4k\}$$

Thus

$$\psi(\tau, k) = \frac{3}{(2+\tau)^3} \qquad \tau \ge 4k$$
$$\psi(\tau, k) = \frac{3}{8(1+2k)^3} \qquad \tau \le 4k \tag{46}$$

In the fourth quadrant ($0 < \tau < 1+k$, $-1 < k < 0$) we have (using (35))

$$\psi(\tau, k) = \frac{9}{L^3}\int_0^{L/2} \mu^2 d\mu = \frac{3}{8} \tag{47}$$

Similarly, in the second quadrant ($0 < k < 1$, $(k-1) < T < 0$), (17) applies, and we have once again

$$\psi(\tau, k) = \frac{3}{8} \tag{48}$$

The probability density within the region $|\tau| \le 1-|k|$, $0 \le |k| \le 1$ is therefore uniform in the second and fourth quadrants but nonuniform in the other two quadrants. In the first and third quadrants the density increases toward the line $\tau = 4k$, and the peak value increases with $|\tau|$ and $|k|$ along the line to the points $\pm(4/5, 1/5)$ on the boundary of the region, where it takes an overall maximum value of $125/72$.

The integrated probability over the whole region $|\tau| \le 1-|k|$, $0 \le |k| \le 1$ is, of course, unity.

The combined probability distribution for T and k can be obtained from (44), (46), (47), and (48) using (40).

4. TWO-PARAMETER REPRESENTATION WITH UNIFORM *A PRIORI* PROBABILITY DENSITY

While the joint probability density of T and k is of interest, our main purpose is to construct an equal-area plot; that is, transform from T, k to new parameters $u(T, k)$, $v(T, k)$ such that the joint *a priori* probability density of u and v is uniform. In fact we may start from the distribution $\psi(\tau, k)$.

In the second and fourth quadrants of the (τ, k) plane, the probability density is already uniform, and so we put

$$u = \tau, \quad v = k \tag{49}$$

for $\tau > 0, k < 0$ and $\tau < 0, k > 0$.

If we now consider the first quadrant, we have two regions: $\tau < 4k$ in region A and $\tau > 4k$ in region B (see Figure 1). In region A (equations (44)), $\psi = 3/(2-\tau)^3$, and in region B, $\psi = 3/(8(1-2k)^3)$. The corresponding density function $\tilde{\psi}$ for u and v is

$$\tilde{\psi}(u, v) = \frac{\psi(\tau, k)}{\left|\dfrac{\partial(u, v)}{\partial(\tau, k)}\right|} \tag{50}$$

where

$$\frac{\partial(u, v)}{\partial(\tau, k)} = \frac{\partial u}{\partial \tau}\frac{\partial v}{\partial k} - \frac{\partial u}{\partial k}\frac{\partial v}{\partial \tau}$$

We choose

$$u = \frac{\tau}{1-\tau/2} \quad v = \frac{k}{1-\tau/2}$$
$$u = \frac{\tau}{1-2k} \quad v = \frac{k}{1-2k} \tag{51}$$

in region A and region B, respectively. This transformation matches on the interface ($\tau = 4k$) of regions A and B and also matches the transformation (49) on the boundaries $\tau = 0$ and $k = 0$.

In region A,

$$\frac{\partial(u, v)}{\partial(\tau, k)} = \frac{1}{(1-\tau/2)^3} \tag{52}$$

and so $\tilde{\psi}(u, v) = 3/8$. Similarly, in region B,

$$\frac{\partial(u, v)}{\partial(\tau, k)} = \frac{1}{(1-2k)^3} \tag{53}$$

and so, once again, $\tilde{\psi}(u, v) = 3/8$.

In the third quadrant, we effect a similar transformation with some changes of sign:

$$u = \frac{\tau}{1+\tau/2} \quad v = \frac{k}{1+\tau/2} \quad \tau > 4k$$
$$u = \frac{\tau}{1+2k} \quad v = \frac{k}{1+2k} \quad \tau < 4k \tag{54}$$

so that $\tilde{\psi}(u, v) = 3/8$ throughout.

The first quadrant in the (τ, k) plane maps onto the first quadrant in the (u, v) plane, and similarly for the other quadrants. In the second and fourth quadrants, of course, the transformation is an identity, and the outer boundaries remain at $v = u \pm 1$ (see Figure 2).

In the first quadrant, the interface between regions A and B is $\tau = 4k$, $u = 4v$, and the boundary $\tau = 1-k$ becomes

$$u = 2(1-v)$$
$$u = 1+v \tag{55}$$

in region A and in region B respectively.

Inverting the transformation (51), we have in region A,

$$k = \frac{v}{1+u/2} \quad \tau = \frac{u}{1+u/2} \quad T = \frac{u}{1+u/2-v} \tag{56}$$

Lines of constant k therefore transform onto lines with slope $k/2$, while lines of constant T become lines with slope $(T-2)/2T$.

In region B,

$$k = \frac{v}{1+2v} \quad \tau = \frac{u}{1+2v} \quad T = \frac{u}{1+v} \tag{57}$$

and lines of constant k remain lines of constant v, while lines of constant T become lines with slope $1/T$, thus effecting a continuous transition with the second quadrant.

The transformation of the third quadrant follows similar lines of course.

We see from Figure 2 that the equal-area plot is a parallelogram with vertices at (0, 1), (4/3, 1/3), (0, –1), and (– 4/3, –1/3). There is no discontinuity in the representation on the u axis, only at the diagonals, $u = 0$ and $u = 4v$.

The probability density over the plot is uniformly 3/8 as we have shown. The total area of the plot is 8/3, giving a total probability of unity, as required.

5. DISCUSSION

Inversions of seismological data giving estimates of the principal moments together with error bars may be displayed on the source type plot to show the range of possible source mechanisms allowed by the data. By this means the results appear in a form which can easily be interpreted in terms of constant-volume and volume change components, and which shows the true proportion of the possible moment tensors that are compatible with the data.

This plot for the parameters T and k of the moment tensor which we have constructed turns out to have a fairly simple character; in fact it is less complex than the compatibility plot which has been set up for the parameters concerned in the measurement of amplitude

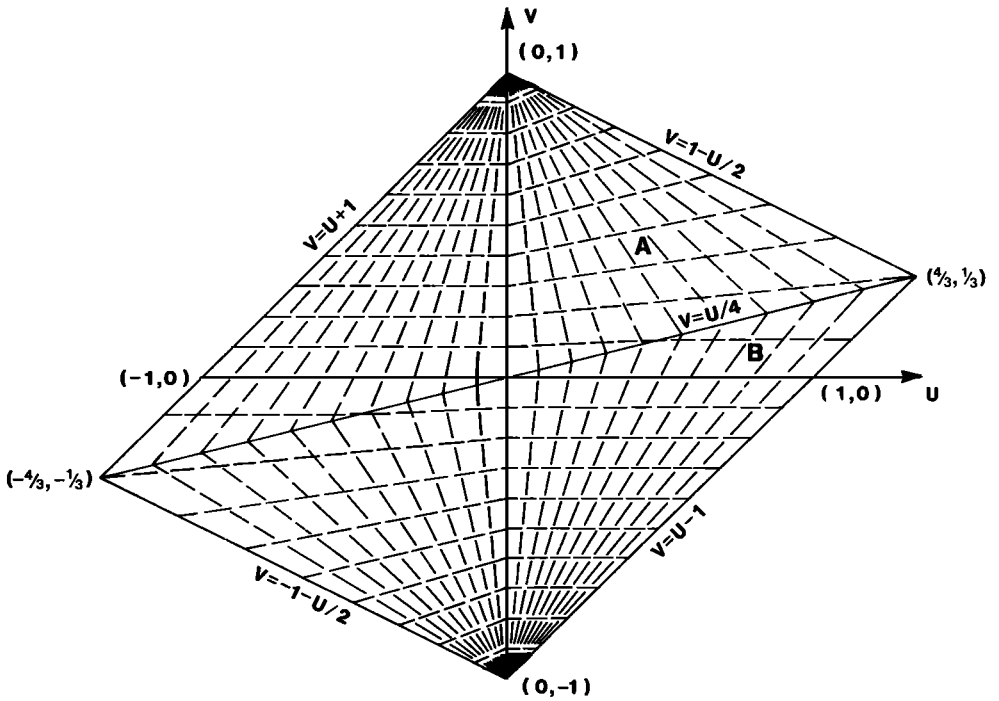

Fig. 2. Equal-area source type plot. Source types are represented using the parameters T and k plotted in the u–v plane, which gives uniform distribution of source types throughout the plot. Lines of equal T (near-vertical) and k (near-horizontal) are shown pecked. The (u, v) coordinates of key points are shown.

ratios of P, pP, and sP [see *Pearce et al.*, 1988]. Figure 2 shows lines of constant k, which measures the relative importance of the dilatational component, and of constant T, which controls the character of the constant-volume component (see (21) and (22)). Figure 3 shows the positions on the plot of some well-known source types.

Purely dilatational sources correspond to $k = \pm 1$ and hence $\tau = 0$. These map onto the two points $(0, \pm 1)$ on the source type plot as shown (Figures 2 and 3). Sources with no dilatation correspond to $k = 0$ and map onto the line $v = 0$ (Figure 2). On this line, T varies from –1 (compensated linear vector dipole) to +1 (negative CLVD). A double couple (or shear crack) plots onto the origin where $T = k = 0$.

A simple linear dipole is given by $T = -1$, $k = 1/3$ (positive) and by $T = 1$, $k = -1/3$ (negative), as shown in Figure 3. The tensile crack also lies on the line $T = -1$ (positive) or $T = 1$ (negative) but it has greater dilatational component than a simple dipole. The exact proportion of dilatation to shear component depends on the elastic parameters of the material in which the source lies; for a Poisson's ratio of 0.25 it plots onto the point (–1, 5/9) as shown.

The distorted shape of the plot obtained can be explained in physical terms. First, the reducing width of the plot toward $k = \pm 1$ is a consequence of the decreasing importance of the constant-volume parameter T, as the proportion of volume change component increases; for the extreme cases $k = \pm 1$, the parameter T is undefined.

Any constant-volume source (i.e., one with $k = 0$) will have positive and negative regions in its far-field P radiation pattern separated by nodal surfaces, which are the familiar nodal planes in the case of the double couple. With increasing dilatational component a preponderance of either negative or positive P radiation develops until a point is reached beyond which the nodal surfaces disappear and the radiation is all of the same polarity. The condition for this boundary is that one of the three principal moments tends to zero. For k positive and increasing, our ordering of the three moments by size (equation (1)) ensures that it is the M_y element that becomes zero last. So from (21) we require

$$\begin{aligned} 2k - 2(1-k) &= 0 \qquad T \geq 0 \\ 2k - (2+T)(1-k) &= 0 \qquad T \leq 0 \end{aligned} \tag{58}$$

For $T \geq 0$ this condition becomes $k = 1/2$ which, by use of (51), becomes

$$v = \frac{u}{4} + \frac{1}{2} \tag{59}$$

For $T \leq 0$ the condition becomes $4k = \tau + 2$, using (28), and using (49) we obtain the same result as (59). Thus we have two segments of the same straight line.

For k negative and decreasing it is the M_x element which becomes zero last, and similar arguments can be used to derive the relationship

$$v = \frac{u}{4} - \frac{1}{2} \tag{60}$$

Thus there are two parallel straight lines on the source type plot (shown by dotted lines in Figure 3) between which nodal surfaces are observed, and outside this region

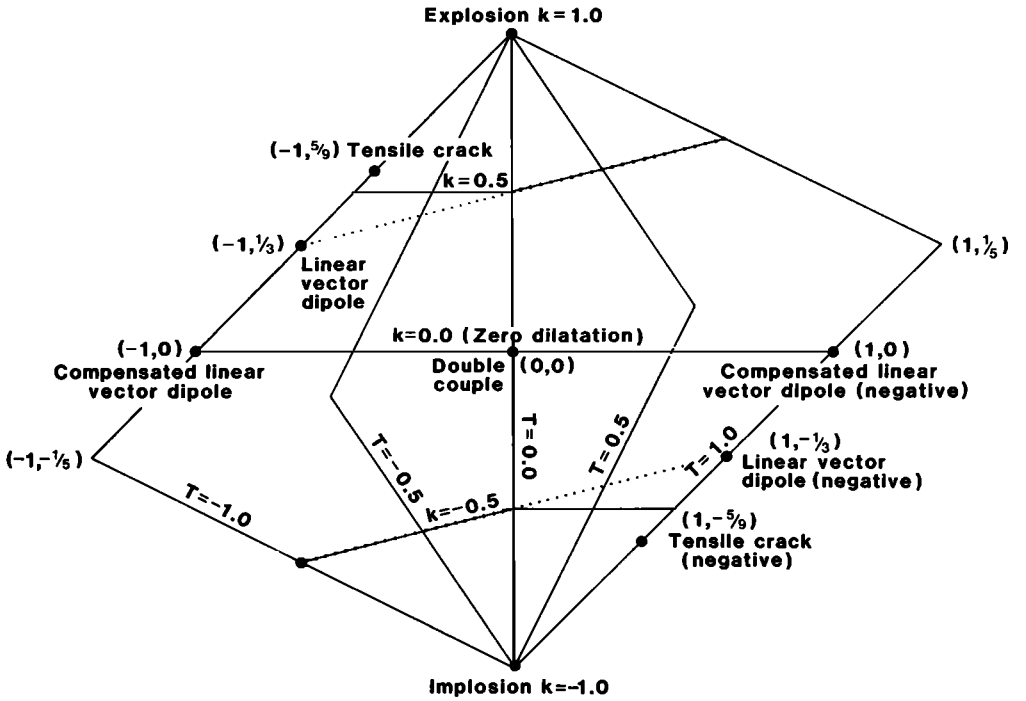

Fig. 3. Equal-area source type plot, showing key points and the positions of key source types in terms of (T, k) coordinates. The dotted lines denote the zone within which nodal surfaces exist in the P wave radiation pattern. Outside this zone, P radiation is all of the same polarity: positive and negative in the upper and lower regions, respectively.

the radiation is either all positive (upper region) or all negative (lower region). These straight lines only follow the lines $k = \pm 1/2$ for one polarity of T because the negative and positive lobes of constant-volume (i.e., $k = 0$) P wave radiation patterns are unequal in amplitude except for $T = 0$ (the double couple). We can see how this fact relates to the shape of the source type plot by considering the extreme case $T = -1$. The radiation pattern then varies as $3\cos^2\theta - 1$, where the direction $\theta = 0$ is its axis of symmetry, giving a positive maximum of 1 along this axis and a negative maximum of $-1/2$ along the toroidal negative lobe normal to this axis. Thus the addition of a smaller proportion of explosive component is required to eliminate the nodal surface than would be required of an implosive component.

We may further ask why the maximum stretching of T values does not occur along the line $k = 0$ ($v = 0$ in Figure 2), but along the line $v = u/4$. We recall that this stretching is a consequence of our equal-area requirement, given uniform distribution of the principal moments, and the maximum stretching corresponds to a small rate of change of these moments as a function of T. For $T = -1$ this maximum occurs when these moments are numerically equal, and this occurs for $k = 0.2$, not $k = 0$. The loci of disappearance of nodal surfaces are also lines of constant rate of change of the principal moments as a function of T. Indeed, the line $v = u/4$ is parallel to these loci (equations (59) and (60)) and exactly bisects the region of the plot where nodal surfaces exist in the P wave radiation pattern (Figure 2).

So far we have restricted attention to the relative sizes of the principal moments of the source. We may go further and estimate the complete range of moment tensors compatible with a given data set by constructing the set of orientations compatible with the data for each source type, according to *Pearce* [1977, 1980], to yield a quantitative measure of the total compatible range in five dimensions. (We recall that the sixth dimension represents the absolute size of the source and has been discarded for our purpose.) A major attraction of this approach to source inversion is that the source type plot on its own provides a direct assessment of the range of compatible source types as a fraction of the total population, and without attention to orientation.

It is important to remember that all source types with $T = \pm 1$, that is on the extreme left- and right-hand edges of the plot (Figure 3), have only two, and not three, degrees of freedom in their orientation, since they have two equal principal moments and thus an axis of symmetry in their radiation patterns which is not characteristic of other source types. Moreover, the purely explosive and implosive source types at $k = \pm 1$ are, of course, symmetrical about all axes. These symmetries do not affect the distribution of source types but are important for the distribution of orientations; we have assumed orientations to have always three degrees of freedom by generalization of the double couple case assumed by *Pearce* [1977]. For a given source type which has $T = \pm 1$ we find that, if any orientation is compatible, then there is always a ribbon of compatible orientations corresponding to rotation of that source type about its axis of symmetry. For a purely explosive or implosive source we find, of course, either that no orientation is compatible or that they all are. The apparent anomaly here is that in such cases the fraction of parameter space allowable is large while only representing a single radiation pattern. The anomaly is, however,

apparent only, since although less information is required to determine the parameters of a source that is assumed *a priori* to have fewer degrees of freedom, it is essential to our approach that no such assumptions are made. If compatible source types are found with a range close to $T = +1$ or -1 the uncertainty in orientation necessarily becomes larger as the symmetrical source type is approached. Similar increasing uncertainty in orientation also occurs as the source type approaches $k = +1$ or -1. The effect corresponds, for instance, to the difficulty of assessing accurately the orientation of a small shear component of an almost completely explosive source.

It is convenient to sample source types at equal intervals of T and k; this is done in the relative amplitude moment tensor program (RAMP) described by *Pearce and Rogers* [this issue]. Each sample point must then be weighted according to the size of the area on the source type plot that it represents, since T and k are, of course, not uniformly distributed on the source type plot. The quantity $\psi(\tau, k)$ calculated from (44), (46), (47), and (48) defines the probability density of source types in the (τ, k) plane and, since the area of any (T, k) increment in the (τ, k) plane is proportional to $(1-|k|)$ (from (40)), the probability density in the (T, k) plane, and thus the weighting factor, is simply $(1-|k|)\ \psi(\tau, k)$.

REFERENCES

Backus, G. E., and M. Mulcahy, Moment tensors and other phenomenological descriptions of seismic sources, I, *Geophys. J. R. Astron. Soc.*, *46*, 341–361, 1976*a*.

Backus, G. E., and M. Mulcahy, Moment tensors and other phenomenological descriptions of seismic sources, II, *Geophys. J. R. Astron. Soc.*, *47*, 301–329, 1976*b*.

Dziewonski, A. M., T. A. Chou, and J. H. Woodhouse, Determination of earthquake source parameters from waveform data for studies of global and regional seismology, *J. Geophys. Res.*, *86*, 2825–2852, 1981.

Fitch, T. J., D. W. McCowan, and N. W. Shields, Estimation of the seismic moment tensor from teleseismic body wave data with application to intraplate and mantle earthquakes, *J. Geophys. Res.*, *85*, 3817–3828, 1980.

Knopoff, L., and M. J. Randall, The compensated linear vector dipole: A possible mechanism for deep earthquakes, *J. Geophys. Res.*, *75*, 4957–4963, 1970.

Pearce, R. G., Fault plane solutions using relative amplitudes of *P* and *pP*, *Geophys. J. R. Astron. Soc.*, *50*, 381–394, 1977.

Pearce, R. G., Earthquake focal mechanisms from relative amplitudes of *P*, *pP* and *sP*: Method and computer program, *AWRE Rep. O 41/79*, Her Majesty's Stationery Office, London, 1979.

Pearce, R. G., Fault plane solutions using relative amplitudes of *P* and surface reflections: Further studies, *Geophys. J. R. Astron. Soc.*, *60*, 459–487, 1980.

Pearce, R. G., and R. M. Rogers, Determination of earthquake moment tensors from teleseismic relative amplitude observations, *J. Geophys. Res.*, this issue.

Pearce, R. G., J. A. Hudson, and A. Douglas, On the use of *P* wave seismograms to identify a double couple source, *Bull. Seismol. Soc. Am.*, *78*, 651–671, 1988.

J. A. Hudson, Department of Applied Mathematics and Theoretical Physics, Silver Street, Cambridge, CB3 9EW, United Kingdom

R. G. Pearce, Department of Geology and Geophysics, University of Edinburgh, James Clerk Maxwell Building, Mayfield Road, Edinburgh, EH9 3JZ, United Kingdom.

R. M. Rogers, Ministry of Defence (Procurement Executive), Blacknest, Brimpton, Reading, Berkshire, RG7 4RS, United Kingdom.

(Received January 30, 1987;
revised December 28, 1987;
accepted July 8, 1988.)